Puustinen et al., http://www.jcb.org/cgi/content/full/jcb.201304012/DC1

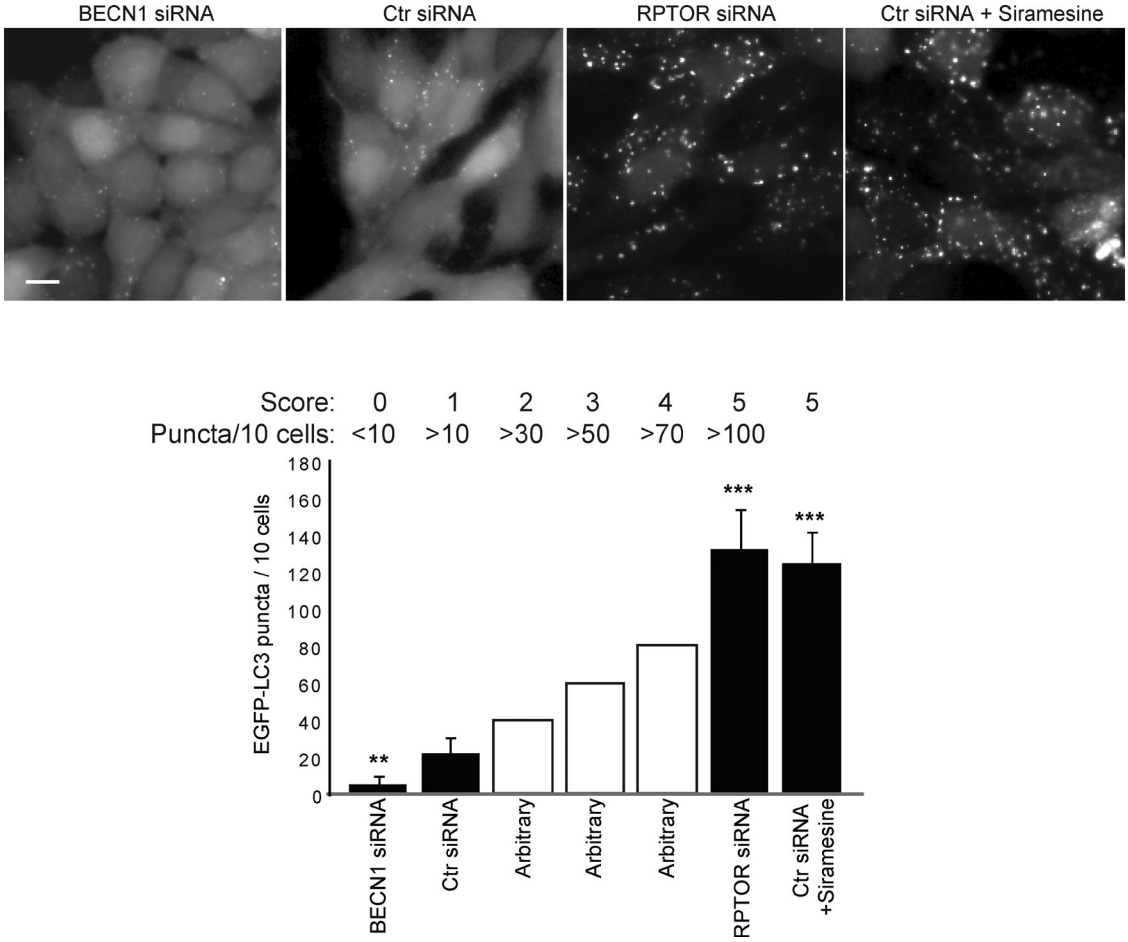

Figure S1. **Scoring system for the siRNA screen.** MCF7-EGFP-LC3 cells were transfected with indicated siRNAs (8 nM), fixed 56 h later, and analyzed for EGFP-LC3 puncta formation. When indicated, 5 µM siramesine was added for the last 3 h. Shown are representative images of the cells (top; bar, 10 µm) and quantification of the number of puncta from a representative experiment (bottom). The values are represented as a mean number of puncta/10 cells ± SDs from four randomly chosen areas of 10 cells. The shown treatments were included as controls to each siRNA screen plate, and they served as the standards for the scoring scale as represented on the bottom figure with a help of three arbitrary values. Ctr, control. **, $P < 0.01$; ***, $P < 0.001$.

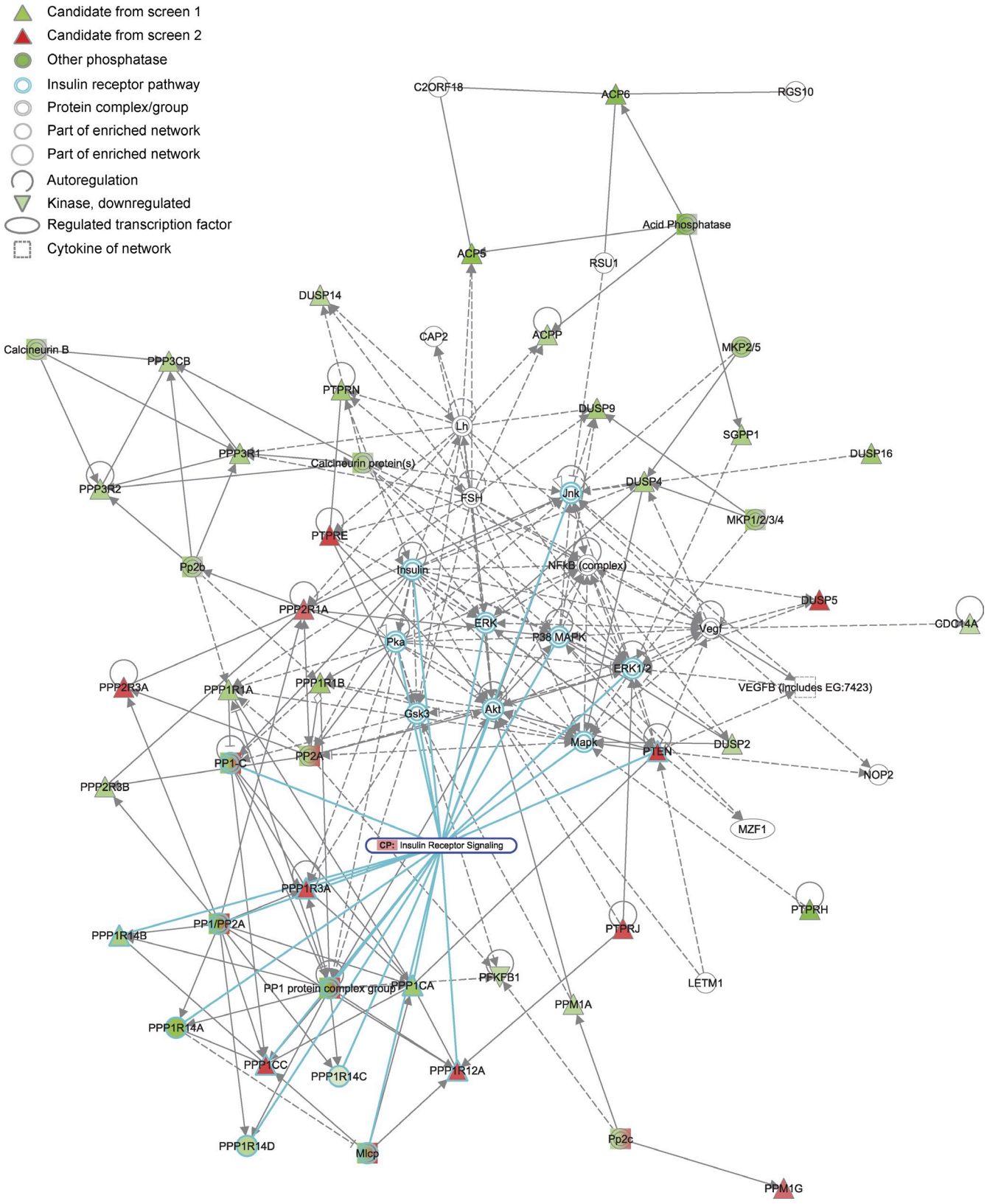

Figure S2. **A cartoon highlighting the positions of the candidate autophagy-regulating genes in the insulin receptor signaling network.** The cartoon was prepared by Ingenuity Pathway Analysis. software. CP, carbohydrate phosphatase; ERK, extracellular signal–regulated kinase; FSH, follicle-stimulating hormone; EG, epidermal growth factor.

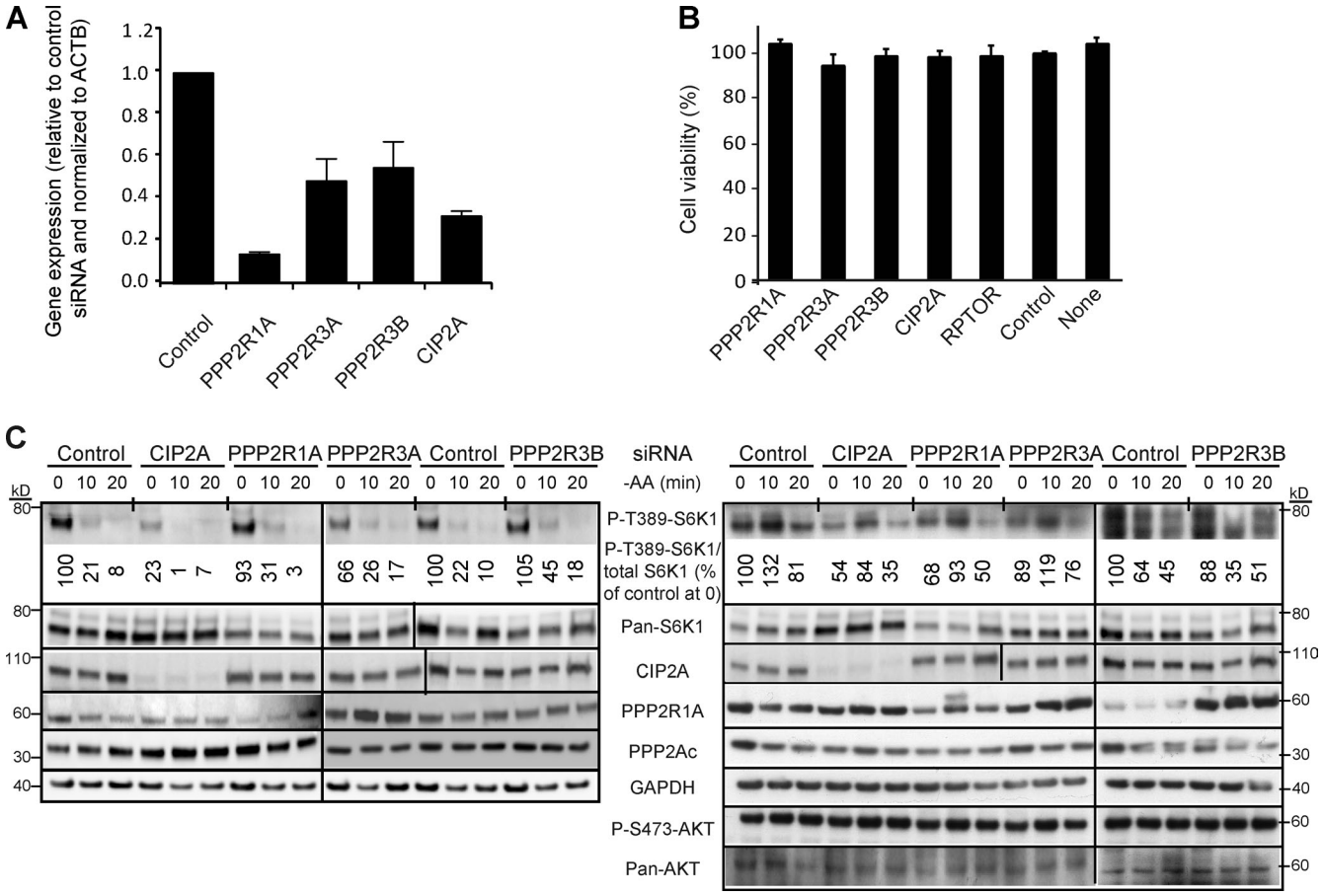

Figure S3. **The effect of siRNAs targeting the autophagy-regulating PP2 subunits on target gene expression, cell density, and mTORC1 pathway.** (A) Total RNA was isolated from MCF7 cells treated with indicated siRNAs (20 nM) for 54 h and analyzed for target gene expression by qPCR using primers designed to specifically amplify the indicated PP2A-related mRNAs and *ACTB* mRNA (internal control). Error bars show SDs for three duplicate experiments. All siRNAs down-regulate their respective targets significantly; $P < 0.01$. (B) The viability of MCF7 cells treated with the indicated siRNAs for 56 h was analyzed by the LDH release assay. The values are expressed as percentages of the density of control siRNA-transfected cells and represent means ± SD of three independent triplicate experiments. (C) Representative immunoblots of the indicated proteins from whole-cell lysates of MCF7 breast carcinoma (left) and U-2-OS osteosarcoma (right) cells treated with the indicated siRNAs for 56 h and subjected to 0–20 min of amino acid starvation (−AA). Long vertical lines separate distinct blots, whereas short vertical lines indicate sites where some lanes have been removed from the same blot.

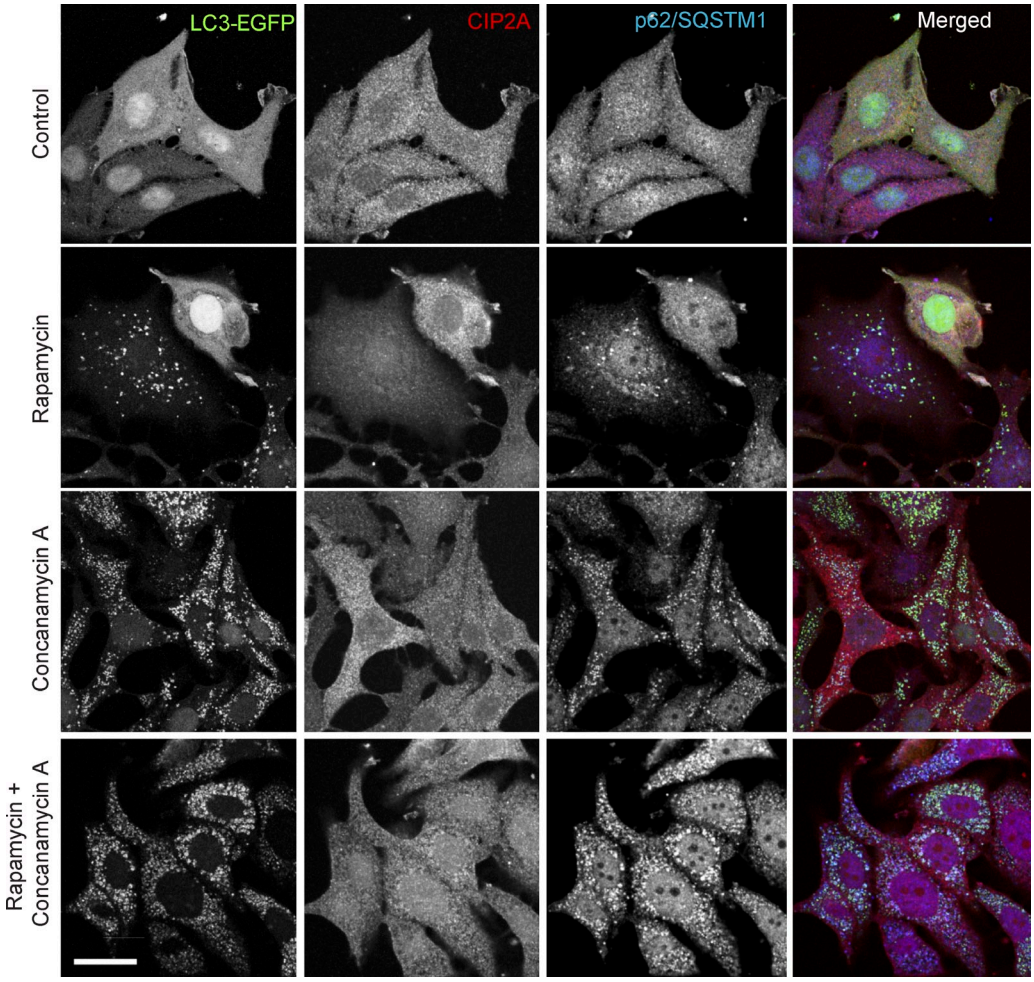

Figure S4. **Colocalization of LC3, p62, and CIP2A.** Representative confocal images of MCF7-LC3-EGFP cells left untreated or treated with 100 nM rapamycin and 2 nM ConA as indicated for 8 h, fixed with formaldehyde, and stained with antibodies against CIP2A and p62/SQSTM1. Bar, 10 µM

Table S1. **List of top candidate genes with highest association with canonical pathways identified by Ingenuity Pathway Analysis**

Ingenuity canonical pathways	−Log (B-H p-value)	Ratio	Molecules
Dopamine receptor signaling	1.39×10^{1}	1.29×10^{-1}	PPP1CC, PPP1R14C, PPP2R1A, PPP1R14D, PPP1R1B, PPP2R3A, PPP1R12A, PPP1R14A, PPP2R3B, PPP1R3A, PPP1CA, PPP1R14B
CDK5 signaling	1.33×10^{1}	1.28×10^{-1}	PPP1CC, PPP1R14C, PPP2R1A, PPP1R14D, PPP1R1B, PPP2R3A, PPP1R12A, PPP1R14A, PPP2R3B, PPP1R3A, PPP1CA, PPP1R14B
Synaptic long-term potentiation	1.24×10^{1}	1.04×10^{-1}	PPP3R2, PPP1CC, PPP1R14C, PPP3CB, PPP1R14D, PPP1R1A, PPP3R1, PPP1R12A, PPP1R14A, PPP1R3A, PPP1CA, PPP1R14B
ERK/MAPK signaling	1.24×10^{1}	6.86×10^{-2}	PPP1CC, PPP1R14C, PPP1R14A, PPP2R3B, PPP1R3A, PPP1R14B, DUSP2, PPP2R1A, DUSP9, PPP2R3A, PPP1R14D, PPP1R12A, DUSP4, PPP1CA
Cardiac β-adrenergic signaling	1.16×10^{1}	7.95×10^{-2}	PPP1CC, PPP1R14C, PPP2R1A, PPP1R14D, PPP1R1A, PPP2R3A, PPP1R12A, PPP1R14A, PPP2R3B, PPP1R3A, PPP1CA, PPP1R14B
Production of nitric oxide and reactive oxygen species in macrophages	9.26	5.82×10^{-2}	PPP1CC, PPP1R14C, PPP2R1A, PPP1R14D, PPP2R3A, PPP1R12A, PPP1R14A, PPP2R3B, PPP1R3A, PPP1CA, PPP1R14B
Breast cancer regulation by stathmin1	8.31	5.24×10^{-2}	PPP1CC, PPP1R14C, PPP2R1A, PPP1R14D, PPP2R3A, PPP1R12A, PPP1R14A, PPP2R3B, PPP1R3A, PPP1CA, PPP1R14B
Insulin receptor signaling	7.44	6.38×10^{-2}	PPP1CC, PPP1R14C, PPP1R14D, PPP1R12A, PPP1R14A, PPP1R3A, PPP1CA, PPP1R14B, PTEN
Protein kinase A signaling	7.43	3.69×10^{-2}	PPP3R2, PPP1CC, PPP1R14C, PPP3CB, PPP1R14D, PPP1R1B, PPP3R1, PPP1R12A, PPP1R14A, PPP1R3A, PPP1CA, PPP1R14B
Riboflavin metabolism	6.14	9.09×10^{-2}	ACP5, ACP6, SGPP1, DUSP16, ACPP
AMPK signaling	3.8	3.57×10^{-2}	PPP2R1A, PFKFB1, PPP2R3A, PPP2R3B, PPM1A, PPM1G
Phospholipase C signaling	3.45	2.69×10^{-2}	PPP3R2, PPP1CC, PPP3CB, PPP3R1, PPP1R12A, PPP1R14A, PPP1CA
ILK signaling	3.11	3.14×10^{-2}	PPP2R1A, PPP2R3A, PPP2R3B, ILKAP, PPP1R14B, PTEN
Cell cycle regulation by BTG family	2.57	8.33×10^{-2}	PPP2R1A, PPP2R3A, PPP2R3B
T cell receptor signaling	2.35	3.64×10^{-2}	PPP3R2, PTPRH, PPP3CB, PPP3R1
Nicotinate and nicotinamide metabolism	2.34	2.94×10^{-2}	ENTPD3, G6PC, NT5C2, DUSP16
iCOS–iCOSL signaling in T helper cells	2.23	3.2×10^{-2}	PPP3R2, PPP3CB, PPP3R1, PTEN
Integrin signaling	2.19	2.44×10^{-2}	PPP1CC, PPP1R12A, ILKAP, PPP1CA, PTEN
Galactose metabolism	2.14	2.61×10^{-2}	G6PC, G6PC2, G6PC3
PI3K/Akt signaling	2.14	2.82×10^{-2}	PPP2R1A, PPP2R3A, PPP2R3B, PTEN
Nur77 signaling in T lymphocytes	2.14	4.69×10^{-2}	PPP3R2, PPP3CB, PPP3R1
cAMP-mediated signaling	2.12	2.3×10^{-2}	PPP3R2, DUSP9, PPP3CB, PPP3R1, DUSP4
Mitotic roles of polo-like kinase	2.1	4.76×10^{-2}	PPP2R1A, PPP2R3A, PPP2R3B
Calcium-induced T lymphocyte apoptosis	2.06	4.23×10^{-2}	PPP3R2, PPP3CB, PPP3R1
PI3K signaling in B lymphocytes	2.06	2.74×10^{-2}	PPP3R2, PPP3CB, PPP3R1, PTEN
GM-CSF signaling	2.05	4.29×10^{-2}	PPP3R2, PPP3CB, PPP3R1
Inositol phosphate metabolism	2.05	2.21×10^{-2}	MTMR14, G6PC, OCRL, PTEN
B cell receptor signaling	1.99	2.55×10^{-2}	PPP3R2, PPP3CB, PPP3R1, PTEN
Chemokine signaling	1.99	4×10^{-2}	PPP1CC, PPP1R12A, PPP1CA
IL-3 signaling	1.97	3.95×10^{-2}	PPP3R2, PPP3CB, PPP3R1
Tight junction signaling	1.9	2.41×10^{-2}	PPP2R1A, PPP2R3A, PPP2R3B, PTEN
Cyclins and cell cycle regulation	1.9	3.37×10^{-2}	PPP2R1A, PPP2R3A, PPP2R3B
Regulation of IL-2 expression in activated and anergic T lymphocytes	1.9	3.33×10^{-2}	PPP3R2, PPP3CB, PPP3R1
Ceramide signaling	1.9	3.33×10^{-2}	PPP2R1A, PPP2R3A, PPP2R3B
Sphingolipid metabolism	1.86	2.68×10^{-2}	SGPP2, SGPP1, DUSP16
Regulation of actin-based motility by Rho	1.86	3.26×10^{-2}	PPP1CC, PPP1R12A, PPP1CA
FXR/RXR activation	1.82	2.88×10^{-2}	G6PC, G6PC2, G6PC3
RANK signaling in osteoclasts	1.8	3.03×10^{-2}	PPP3R2, PPP3CB, PPP3R1
CTLA4 signaling in cytotoxic T cells	1.77	2.97×10^{-2}	PPP2R1A, PPP2R3A, PPP2R3B
Starch and sucrose metabolism	1.77	1.55×10^{-2}	G6PC, G6PC2, G6PC3
Glycolysis/gluconeogenesis	1.69	2.04×10^{-2}	G6PC, G6PC2, G6PC3
Regulation of eIF4 and p70S6K signaling	1.64	2.22×10^{-2}	PPP2R1A, PPP2R3A, PPP2R3B

B-H, Benjamini and Hochberg (1995) adjusted; ERK, extracellular signal–regulated kinase; iCOS, inducible T cell co-stimulator; iCOSL, inducible T cell co-stimulator ligand; ILK, integrin-linked kinase; GM-CSF, granulocyte-macrophage colony-stimulating factor; FXR, farnesoid X receptor; RXR, retinoid X receptor; RANK, receptor activator of nuclear factor κB.

Reference

Benjamini, Y., and Y. Hochberg. 1995. Controlling the false discovery rate: a practical and powerful approach to multiple testing. *J. R. Stat. Soc. Ser. B Stat. Methodol.* 57:289–300.